Benavente Martínez, R.; Salvador Moya, MD.; Alcázar, M.; Moreno, R. (2012). Dense nanostructured zirconia compacts obtained by colloidal filtration of binary mixtures. Ceramics International. 38(3):2111-2117. doi:10.1016/j.ceramint.2011.10.051.

Dense nanostructured zirconia compacts obtained by colloidal filtration of binary mixtures

R. Benavente[1], M. D. Salvador[1], C. Alcazar[2], R. Moreno[2]

[1]Instituto de Tecnología de Materiales, Universitat Politècnica de València, 46022 Valencia, Spain.

[2]Instituto de Cerámica y Vidrio, CSIC, Kelsen 5, 28049 Madrid, Spain.

Abstract

As starting materials two commercial nanosized zirconias doped with 3 mole% of Y_2O_3 were used: a powder of about 100 nm (TZ3YE, Tosoh, Japan) and a colloidal suspension of about 15 nm (Mel Chemicals, UK). Colloidal stability in water was studied for both zirconias in terms of zeta potential as a function of deflocculant concentration and pH. Concentrated suspensions were prepared by dispersing the powder in the colloidal suspension to solids loadings ranging from 5 to 30 vol.% using a sonication probe to achieve dispersion. The rheological behavior was optimized in terms of solids content, deflocculant content and sonication time. Optimized suspensions with up to 25 vol.% solids showed a nearly Newtonian behavior and extremely low viscosities and maintain stable for long times (days) which is an important drawback of conventional nanoparticle suspensions. Samples obtained by slip casting in plaster moulds were used for dynamic sintering studies and dense, nanostructured specimens were obtained at temperatures of 1300-1400ºC.

Keywords: Y-TZP, Suspensions, Rheology, Nanoparticles

Introduction

Yttria stabilized tetragonal zirconia polycrystalline (YTZP) ceramics are used in a variety of structural and functional applications due to their high strength, high toughness and good wear resistance over a wide temperature range.[1-3] As a biomaterial

the most important application of Y-TZP was related to the manufacture of ball heads for total hip replacement, although this application has been stopped and it has received a growing interest for dental applications.[4,5]

Y-TZP ceramics belong to the family of transformation toughened ceramics,[6,7] which main feature consists in a microstructure completely formed by metastable tetragonal grains at room temperature that can undergo transformation to monoclinic. This is accomplished by a volume increase of 3-4 vol.%, which is the origin of a compressive stress field that operates inversely to the tensile stress that leads the crack and stops it. Factors affecting the phase transformation volume are the grain size of the tetragonal phase, the amount of stabilizer, and the restraining conditions.[8-10] One important feature of Y-TZP is the superplasticity, that is, the capacity of a polycrystal to support great elongation at high temperature and low stress.[11,12]

TZP materials were largely studied over the 80's and 90's, where the main objective was to obtain fully dense tetragonal zirconia at typical temperatures of 1400º-1500ºC. Typical grain sizes of the sintered materials were by 0.5-2.0 μm, depending on sintering temperature, holding time, and physicochemical properties of the starting powders.[8,9,13,14] Fracture toughness as high as 12-14 MPa.m$^{1/2}$ were obtained and hardness values were by 12-14 GPa.

Moreover, a great effort was devoted to the production of pure and controlled Y-TZP powders in order to obtain dense, fine grained materials at lower sintering temperatures. Different chemical routes, such as sol-gel technology, coprecipitation methods, etc., were optimized to achieve dense materials by pressureless sintering methods.[15,16] Nanostructured ceramics display a range of enhanced properties compared to those obtained with submicrometer counterparts.[17,18] However the processing of nanopowders and its further densification to obtain nanostructured dense is difficult because of the strong tendency to agglomeration and spontaneous grain growth during sintering.[19,20] To overcome the densification problems pressure assisted sintering techniques have been used, such as hot pressing, and more recently, electric field-assisted sintering (FAST), also known as spark plasma sintering (SPS)[21,22] Other authors have investigated the possibility of using two-step sintering to achieve high densities while maintaining fine grain sizes.[23-25]

Colloidal processing is a powerful way for the processing of nanoparticles that can be maintained far apart each other using deflocculants that help to control the interparticle forces during all processing stages.[26-28] Thus, the colloidal approach has

demonstrated its suitability for the production of uniform, dense green bulk bodies from nanopowders.[29,30]

The synthesis and colloidal processing of nanozirconia powders has been largely studied.[31-35] Some of these studies have reported the isoelectric point of different powders and the effect of different kinds of deflocculants on the stability, as well as the rheological behavior of concentrated suspensions. In these studies, the dispersion with anionic polyelectrolytes like those based on polyacrylic acid,[32,33] cationic polyelectrolytes like polyethylenimine,[34] or rhamnolipid biosurfactants,[35] for example, have been described in detail for different nanozirconias with average sizes ranging from 15 to 60 nm.

The aim of this work was to study the colloidal processing and the rheological behavior of concentrated bimodal suspensions consisting of a mixture of a commercial nanosized powder of Y-TZP and a colloidal suspension of undoped zirconia to produce homogeneous green bodies with high density by slip casting. The obtained compacts were sintered to high density while maintaining controlled grain size.

Experimental

As starting materials two commercial nanosized zirconias doped with 3 mole% of Y_2O_3 were used: a powder (TZ3YE, Tosoh, Japan), and a colloidal suspension (Mel Chemicals, UK). The former is a powder supplied in the form of spherical granules with a typical diameter below 100 nm. The last is formed by nanoparticles of 15 nm and it is supplied as an aqueous colloidal suspension with pH ~ 3, and a solids content of 5 vol.% (23 wt%).

The physicochemical characteristics of the TZ3Y powder are the following. The specific surface area, determined using the single-point BET method ((Monosorb Surface Area Analyser, MS-13, Quantachrome Corporation, Boynton Beach, USA) after degassing at 150 ºC, was 14.5 ± 0.5 m^2/g. The density (measured by He-pycnometry, with a Multipycnometer, Quantachrome Co., USA), was 5.9 ± 0.2 g/cm^3. The BET diameter calculated from the surface area was 70 nm. The colloidal suspension contains particles with an average particle size of 15 nm, and the specific surface area of dried powders was ~15 m^2/g. The thermo-gravimetric analysis of the TZ3Y nanopowders revealed a weight loss of ~ 0.5%, whereas the dry solids obtained

from the colloidal suspension revealed a weight loss of ~ 6%, thus demonstrating the presence of some organic additive that could difficult the adsorption of deflocculants. The morphology of the as-received powder was observed by field emission gun scanning electron microscopy (FE-SEM, Hitachi S-4700 type I, Tokyo, Japan), and transmission electron microscopy (TEM, H7100, Hitachi, Japan). The crystalline phases were identified by X–ray Diffraction (XRD) (Bruker D8 Advance, Karlsruhe, Germany) and using the Garvie's approach the ratio of tetragonal phase (density = 6.07 g/cm^3, ASTM 83-113) and monoclinic phase (density = 5.82 g/cm^3, ASTM 37-1484), was found to be 82/18 the resulting density being 6.01 g/cm^3. Thermogravimetric analysis was performed using a Netzsch apparatus (STA 409, Germany).

All suspensions were prepared in deionised water. The colloidal stability of the nanosuspensions was studied measuring the zeta potential as a function of pH using a Zetasizer NanoZS instrument (Malvern, UK), based in the laser Doppler velocimetry technique. Different dilutions were tested to measure the zeta potential with the best accuracy, which was reached for a concentration of 0.01 wt%, using KCl 10^{-2} M as inert electrolyte. pH values were determined with a pH-meter (716 DMS Titrino, Metrohm, Switzerland) and were adjusted with HCl and KOH solutions (10^{-2} M). To improve the dispersion state, some sonication times were tested using an ultrasounds probe (UP 400S, Dr. Hielscher GmbH, Germany) in order to avoid agglomerates. A sonication time of 2 min was used for the preparation of diluted suspensions for zeta potential measurements.

According to previous tests, the TZ3Y suspension can be prepared to high solids loadings without any deflocculant. However, to enhance the dispersion of the powder in the colloidal suspension a polyacrylic-acid based deflocculant (Duramax D3005, Rohm & Haas, USA) was successfully added to concentrations of 1, 2, and 3 wt% on a dry solids basis.

The rheological behaviour of the TZ3Y nanopowder was optimized for a solids loading of 30 vol.% (72 wt%). Then, suspensions of the mixtures (Mel + Tosoh) were prepared by adding the TZ3Y nanopowder into the colloidal suspension to final solids loadings of 10, 15, 20, 25, and 30 vol.% (i.e. 40, 51, 60, 66, and 72 wt.%, respectively). The rheological behaviour of these nanosuspensions was determined using a rheometer (Haake RS50, Thermo, Karlsruhe, Germany) operating at controlled shear rate (CR) by loading the shear rate from 0 to 1000 s^{-1} in 5 min, maintaining at 1000 s^{-1} for 1 minute

and uploading from 1000 to 0 in 5 min. The measurements were performed at 25ºC using a double-cone and plate system.

These suspensions were slip cast in plaster moulds to obtain discs with 20 mm in thickness. Green densities were measured by Hg immersion after drying for 48 h. Static sintering experiments were done to temperatures of 1300, 1350 and 1400ºC with heating and cooling rates of 5ºC/min. The annealing time selected was 2h. The microstructures of diamond polished (down to 1 μm) samples were characterized by field emission gun-scanning electron microscopy. The crystallinity of the sintered specimens was determined by X-ray diffraction (XRD) (Bruker Advance D8, USA) with Cu Kα radiation. The sintered density was measured by Archimedes' method in water.

Results and discussion

Figure 1 shows the morphology of the starting powders observed by TEM. The colloidal suspension shows regular, well-dispersed particles of nanometric size and without large agglomerates. The powder TZ3Y is supplied in the form of spherical granules with nanometric size (< 100 nm) in good agreement with the calculated BET mean diameter. TEM pictures show that primary particles are readily dispersed with some small agglomerates formed by several units.

The variation of zeta potential of TZ3Y powders as a function of pH is shown in figure 2 for suspensions dispersed with different concentrations of deflocculant. The isoelectric point (IEP) occurs at pH 3.2, and the zeta potential values are higher than 30 mV at pH > 7. The addition of PAA shifts the isoelectric point very slightly, until pH 2.6 for 3 wt% PAA. However, high absolute zeta potential values are reached at pH ≥ 4.

The variation of zeta potential versus pH for the colloidal suspension (MEL) without PAA and with PAA contents of 1, 2, and 3 wt% is shown in figure 3. The isoelectric point without adsorbed deflocculant occurs at pH 6.5, and decreases to near 6, 3.5, and 2.5 for 1, 2, and 3 wt% PAA, respectively. In addition to zeta potential, the particle size distribution of the colloidal suspensions was determined for all dispersing conditions. Figure 4 shows the variation of average size as a function of pH for suspensions prepared with different PAA contents. It can be observed that for any deflocculant content the particle size strongly increases at a pH value that corresponds very accurately with the corresponding IEP. This illustrates the agglomeration of

particles occurring at the vicinity of the IEP. It is also observed that the values of these maxima are lower as the PAA content increases thus demonstrating that the agglomeration level is lower for higher PAA concentration.

Concentrated suspensions of TZ3Y powder were prepared to solids loadings of 30 vol.% without PAA and with 1 wt% PAA. For both concentrations the effect of sonication time on suspension stability was studied. Figures 5 and 6 show the flow curves of suspensions without and with PAA, respectively, homogenized by mechanical mixing without ultrasounds first, and with sonication times of 2, 4, and 6 min. In both cases there is a similar tendency according to which the suspensions prepared without ultrasounds exhibit a high viscosity and a broad thixotropic cycle, demonstrating that these suspensions have a complex behavior and particles develop some structure at rest. The application of ultrasounds strongly reduces both the viscosity and the time dependency, which becomes negligible in the case of suspensions without PAA. The comparison of both figures clearly shows that the addition of PAA increases both the viscosity and the thixotropy, that is, it has a deleterious effect on the suspensions stability.

According to these results concentrated suspensions of mixtures of both types of zirconia (colloidal and powder) were prepared without any deflocculant addition. Suspensions were prepared by adding TZ3Y powder to the colloidal suspension. The colloidal suspension has a solids content of 5 vol.% and TZ3Y powder was added until total zirconia concentrations of 10, 15, 20, and 30 vol.%. As in the case of TZ3Y suspensions the effect of sonication on the rheological behavior was studied. Figures 7 and 8 show the flow curves for the different solids loading for as-prepared suspensions without sonication and the same suspensions homogenized with 2 min US.

Suspensions prepared by mechanical mixing without sonication had some thixotropy above solid concentrations of 15 vol.%. However, optimized suspensions, i.e. those prepared with 2 min sonication, showed a nearly Newtonian behavior, excepting the most concentrated one that exhibited a shear thinning response with a broad thixotropic cycle. In spite of the high solids loadings achieved for these suspensions of nanoparticles viscosities are extremely low, thus facilitating shape forming. It is worthy to note that the pH value increased progressively from 2.8 to 5.2 as the solids loading increased from 5 to 30 vol.%, but the application of ultrasounds did not change the pH.

From these curves it is possible to draw the variation of viscosity with solids loading, as it is shown in figure 9 for suspensions with and without sonication. Viscosity values were taken at a shear rate of 1000 s^{-1}, which can be assimilated to infinite shear rate extrapolation. The non-sonicated suspensions show an increase of viscosity at very low solids loadings, whereas suspensions sonicated for 2 min maintain very low viscosity until the maximum solids loading, where a sharp increase is also detected.

Sonication has an important effect on the rheological behavior of the suspensions and changes significantly their aging behavior. Figure 10 compares the variation of viscosity with aging time for suspensions with 25 vol.% solids prepared without and with 2 min sonication. Viscosity significantly increases for non-sonicated suspensions but maintains nearly constant for sonicated suspensions, thus meaning that the stability of these suspensions is preserved for longer times. This is an important point as it is frequently observed that concentrated suspensions of nanoparticles destabilize after short aging times of even a few hours.

These suspensions were slip cast and dried before sintering tests. The green density of the cast bodies seems to slightly increase with solids content from 55% to 56.8% of theoretical. In figure 11 the FEG-SEM microstructure of specimens treated at temperatures of 1300º, 1350º, and 1400ºC are shown. The XRD patterns for the sintered specimens showed that tetragonal phase was the unique phase detected, Y-TZP. The particle size maintains in the nanometer size region, but a clear tendency to coarsening with increasing sintering temperature is observed. The average grain size (evaluated by the intercepting line method) increases from 160 ± 15 nm to 180 ± 30 nm and 230 ± 60 nm for temperatures of 1300º, 1350º and 1400ºC. As it can be seen not only the average size but also the deviation increases, that is, the distribution becomes broader as coarse grains are being formed at expenses of the smallest grains.

Conclusions

The preparation of dense Y-TZP nanostructured ceramics has been studied using two nanosized zirconia powders with different particles sizes. The colloidal stability was studied through zeta potential measurements using diluted suspensions and optimizing the rheological behavior of concentrated suspensions in terms of deflocculant contents, pH and sonication time. Suspensions of the mixtures were

prepared by adding the TZ3Y nanopowder into the colloidal suspension up to final solids loadings of 30 vol.% (i.e. 72 wt.%) using 2 min sonication time and then cast into plaster moulds. Dense specimens with controlled size and homogeneous microstructure were obtained after sintering at temperatures of 1300º, 1350º and 1400ºC.

Acknowledgements

This work has been supported by Spanish Ministry of Science and Innovation (Projects MAT2009-14144-C03-02 and MAT2009-14369-C02-01). R Moreno thanks to Universidad Politécnica de Valencia for the concession of a grant in the frame of its Programme of Support to R+D (PAID-02-11, R-1752).

References

1. R. C. Garvie, ‘‘Structural applications of ZrO_2-bearing materials,’’ Zirconia II., Adv. Ceram., Vol 12, ed. N. Claussen, et al. American Ceramic Society, Westerville, OH, 465–478, (1984).
2. B. Basu, J. Vleugels, and O. van der Biest, “Toughening tailoring of yttria-doped zirconia ceramics”, Mater. Sci. Eng. A, 380 (1-2) 215-221 (2004).
3. A. G. Evans, “Perspective on the development of high-toughness ceramics”, J. Am. Ceram. Soc. 73, 187-206 (1990).
4. J. Chevalier, A. H. De Aza, G. Fantozzi, M. Schehl, and R. Torrecillas, “Extending the lifetime of ceramic orthopaedic implants”, Adv. Mater., 12, 1619–1621 (2000).
5. C. Piconi, W. Burger, H. G. Richter, A. Cittadini, G. Maccauro, V. Covacci, N. Bruzzese, G. A. Ricci, and E. Marmo, “Y-TZP ceramics for artificial joint replacements”, Biomaterials, 19, 1489-1494 (1998).
6. N. Claussen, ‘‘Microstructural design of zirconia-toughened ceramics (ZTC),’’ zirconia II., Adv. Ceram., Vol 12, ed. N. Claussen, et al. American Ceramic Society, Westerville, OH, 325–351, (1984).
7. M. Ruhle and A. H. Heuer, ‘‘Phase transformations in ZrO_2 containing ceramics: II, The martensitic reaction in t-ZrO_2,’’ Zirconia II., Adv. Ceram., Vol 12, ed. N. Claussen, et al. American Ceramic Society, Westerville, OH, 14–32, (1984).

8. F. F. Lange, “Transformation-toughened ZrO_2: correlation between grain size control and composition in the system ZrO_2-Y_2O_3”, J. Am. Ceram. Soc., 69 (3) 240-242 (1986).
9. R. H. J. Hannik, P. M. Kelly, and B. C. Muddle, “Transformation toughening in zirconia containing ceramics”, J. Am. Ceram. Soc., 83 [3] 461–487 (2000).
10. B. Basu, J. Vleugels, and O. van der Biest, “Transformation behaviour of tetragonal zirconia. Role of dopant content and distribution”, Mater. Sci. Eng. A, 366 (2) 338-347 (2004).
11. F. Wakai, S. Sakaguchi, and Y. Matsuno, “Superplasticity of yttria-stabilized tetragonal ZrO_2 polycrystals”, Adv. Ceram. Mater. 1, 259-263 (1986).
12. M. Jimenez-Melendo, A. Dominguez-Rodriguez, A. Bravo-Leon, “Superplastic flow of fine-grained Y_2O_3-stabilized ZrO_2 polycrystals. Constitutive equation and deformation mechanisms”, J. Am. Ceram. Soc., 81, 2761-76 (1998).
13. R. A. Cutler, J. R. Reynolds, and A. Jones, “Sintering and characterization of polycrystalline monoclinic, tetragonal, and cubic zirconia”, J. Am. Ceram. Soc., 75 (8) 2173-2183 (1992).
14. T. K. Gupta, J. H. Bechtold, R. C. Kuznickie, L. H. Cadoff, and B. R. Rossing, “Stabilization of tetragonal phase in polycrystalline zirconia”, J. Mater. Sci., 12 (12) 2421-2426 (1977).
15. C. J. Brinker, D. E. Clark, and D. R. Ulrich (eds), “Better ceramics through chemistry”, Mat. Res. Soc. Proc., vol 32, North-Holland, New York (EEUU) 1984.
16. P. Durán, M. Villegas, J. F. Fernández, F. Capel, and C. Moure, “Theoretically dense and nanostructured ceramics by pressureless sintering of nanosized Y-TZP powders”, Mater. Sci. Eng. A, 232 (1) 168-176 (1997).
17. M Mayo, “Processing of nanocrystalline ceramics from ultrafine particles”, Int. Mater. Rev., 41, 85-115 (1996).
18. M. A. Meyers, A. Mishra, and D. J. Benso, “Mechanical properties of nanocrystalline materials”, Prog. Mat. Sci., 51, 427-556 (2006).
19. J. G. P. Binner and B. Vaidhyanathan, “Processing of bulk nanostructured ceramics”, J. Eur. Ceram. Soc., 28, 1329-33 (2008).
20. J. R. Groza, “Sintering of nanocrystalline powder”, Int. J. Powder Metall., 35 (7) 59-66 (1999).

21. D. Yang, R. Raj, and H. Conrad, “Enhanced sintering rate of zirconia (3Y-TZP) through the effect of a weak dc electric field on grain growth”, J. Am. Ceram. Soc., 93 (10) 2935-2937 (2010).
22. J. Langer, M. J. Hoffmann, and O. Guillon, “Electric field assisted sintering in comparison with the hot pressing of yttria stabilized zirconia”, J. Am. Ceram. Soc., 94 (1) 24-31 (2011).
23. C. Robert, F. Ansart, C. Deloget, M. Gaudon, and A. Rousset, Dense yttria stabilized zirconia: sintering and microstructure”, Ceramics int., 29 (2) 151-158 (2003).
24. X. H. Wang, P. L. Chen, and I. W. Chen, “Two-step sintering of ceramics with constant grain size: I: Y2O3”, J. Am. Ceram. Soc., 89 (2) 431-437 (2006).
25. J. Binner, K. Annapoorani, A. Paul, I. Santacruz, and B. Vaidhyanathan, “Dense nanostructured zirconia by two stage conventional/hybrid microwave sintering”, J. Eur. Ceram. Soc., 28, 973-7 (2008).
26. F. F.Lange, “Powder processing science and technology for increased reliability”, J. Am. Ceram. Soc., 72 (91) 3–15 (1989).
27. R. Moreno, “The role of slip additives in tape casting technology. I: solvents and dispersants”, Am. Ceram. Soc. Bull., 71 (10) 1521-1531 (1992).
28. W. M. Sigmund, N. S. Bell, and L. Bergström, “Novel powder-processing methods for advanced ceramics”, J. Am. Ceram. Soc., 83(10) 1557–1574 (2000).
29. I. Santacruz, M. I. Nieto, J. Binner, and R. Moreno, “Gel casting of aqueous suspensions of BaTiO3 nanopowders”, Ceram. Int., 5, 321–326 (2009).
30. L. P. Meier, L. Urech, and L. J. Gauckler, “Tape casting of nanocrystalline ceria gadolinia powder”, J. Eur. Ceram. Soc., 24, 3753–3758 (2004).
31. O. Vasylkiv and Y. Sakka, “Synthesis and colloidal processing of zirconia nanopowder”, J. Am. Ceram. Soc., 84 (11) 2489–2494 (2001).
32. I. Santacruz, K. Anapoorani, and J. G. P. Binner, “Preparation of high solids content nanozirconia suspensions”, J. Am. Ceram. Soc., 91 (2) 398-405 (2008).
33. B. P. C. Ragupathy and J. G. P. Binner, “Spray granulation of nanometric zirconia particles”, J. Am. Ceram. Soc., 94 (1) 42-48 (2011).
34. J. Wang, L. Gao, Adsorption of polyethylenimine on nanosized zirconia particles in aqueous suspensions, J. Colloid Interface Sci., 216, 436-439 (1999).

35. M. Biswas and A. M. Raichur, “Electrokinetic and rheological properties of nano zirconia in the presence of rhamnolipid biosurfactant”, J. Am. Ceram. Soc., 91 (19) 3197-3201 (2008).

Captions to figures

Figure 1. Morphology of the starting zirconia powders as observed by transmission electron microscopy: a) colloidal zirconia Mel, b) Y-TZP powder Tosoh

Figure 2. Variation of zeta potential of TZ3Y suspension (Tosoh) as a function of pH for suspensions dispersed with different concentrations of deflocculant.

Figure 3. Variation of zeta potential of colloidal zirconia (Mel) as a function of pH for suspensions dispersed with different concentrations of deflocculant.

Figure 4. Variation of mean particle size of colloidal zirconia (Mel) as a function of pH for suspensions dispersed with different concentrations of deflocculant.

Figure 5. Flow curves of 30 vol.% suspensions of TZ3Yzirconia (Tosoh) without deflocculant prepared without and with sonication for 2, 4, and 6 min.

Figure 6. Flow curves of 30 vol.% suspensions of TZ3Yzirconia (Tosoh) with 1 wt% of deflocculant prepared without and with sonication for 2, 4, and 6 min.

Figure 7. Flow curves suspensions of mixtures of TZ3Yzirconia (Tosoh) and colloidal zirconia (MEL) prepared without sonication to different solids loadings (5-30 vol.%).

Figure 8. Flow curves suspensions of mixtures of TZ3Yzirconia (Tosoh) and colloidal zirconia (MEL) prepared with 2 min sonication to different solids loadings (5-30 vol.%).

Figure 9. Variation of high shear viscosity of suspensions of the mixtures as a function of solids loading, as-prepared and after 2 min sonication.

Figure 10. Variation of viscosity with aging time for suspensions with 25 vol.% solids prepared without and with 2 min sonication.

Figure 11. FEG-SEM microstructure of cast specimens sintered at temperatures of 1300ºC (a), 1350ºC (b), and 1400ºC (c).

Figure
Click here to download high resolution image

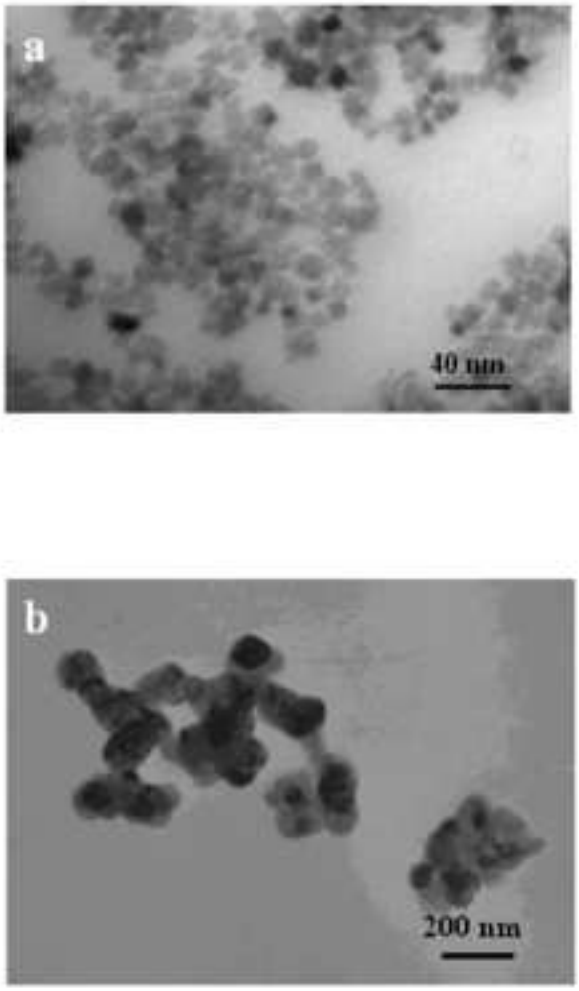

Figure 1. Morphology of the starting zirconia powders as observed by transmission electron microscopy: a) colloidal zirconia Mel, b) Y-TZP powder Tosoh

Figure

Click here to download high resolution image

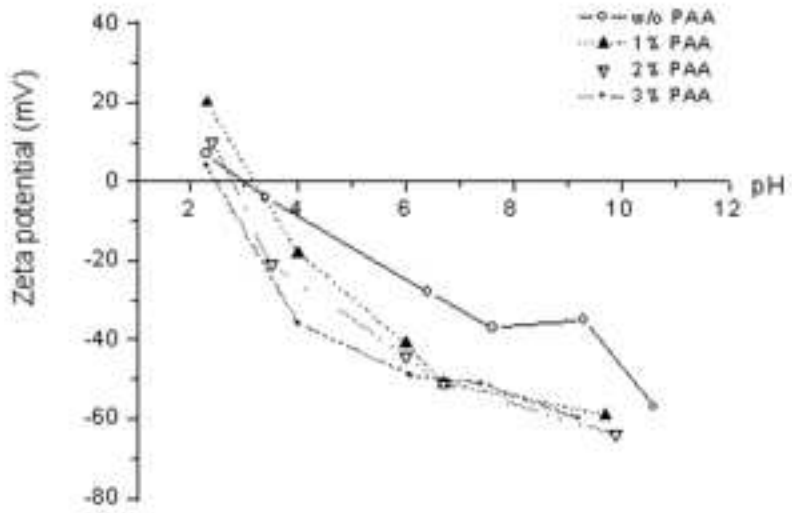

Figure 2. Variation of zeta potential of TZ3Y suspension (Tosoh) as a function of pH for suspensions dispersed with different concentrations of deflocculant.

Figure
Click here to download high resolution image

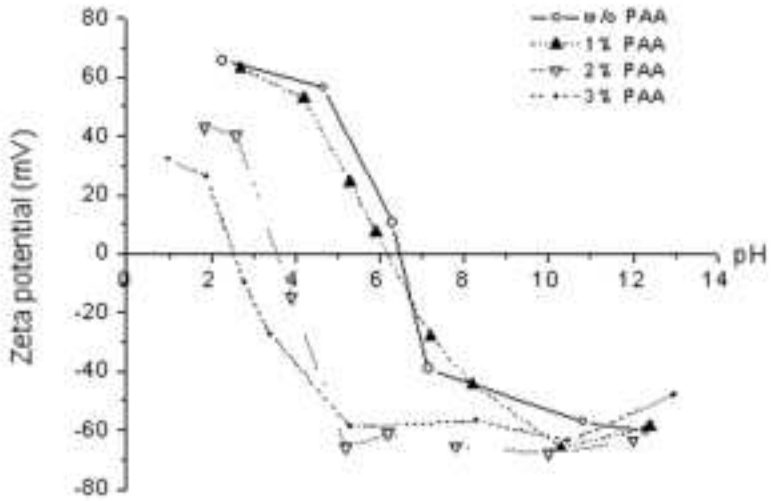

Figure 3. Variation of zeta potential of colloidal zirconia (Mel) as a function of pH for suspensions dispersed with different concentrations of deflocculant.

Figure
Click here to download high resolution image

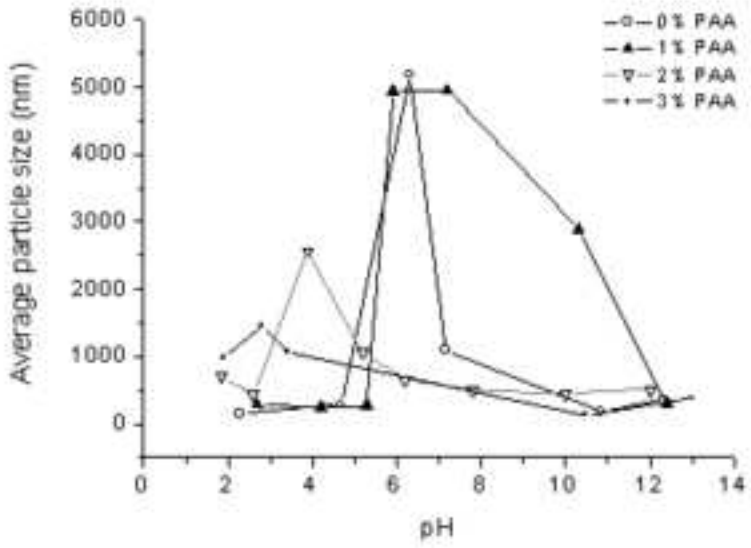

Figure 4. Variation of mean particle size of colloidal zirconia (Mel) as a function of pH for suspensions dispersed with different concentrations of deflocculant.

Figure

Click here to download high resolution image

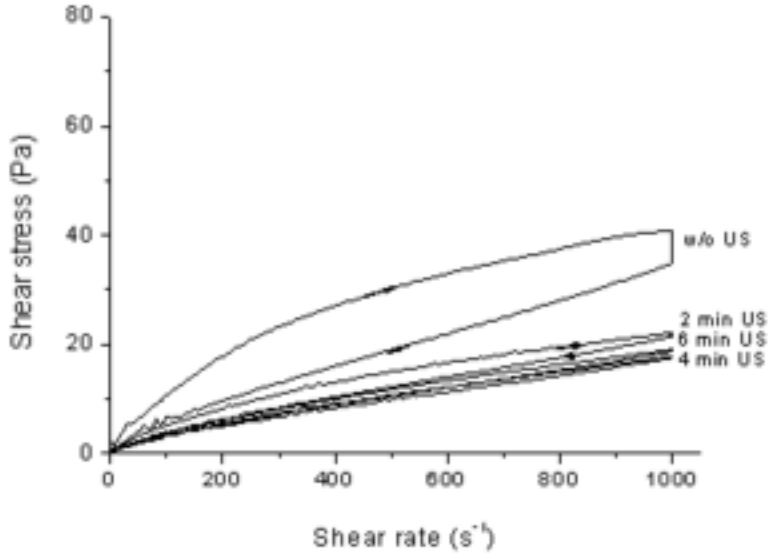

Figure 5. Flow curves of 30 vol.% suspensions of TZ3Y zirconia (Tosoh) without deflocculant prepared without and with sonication for 2, 4, and 6 min.

Figure
Click here to download high resolution image

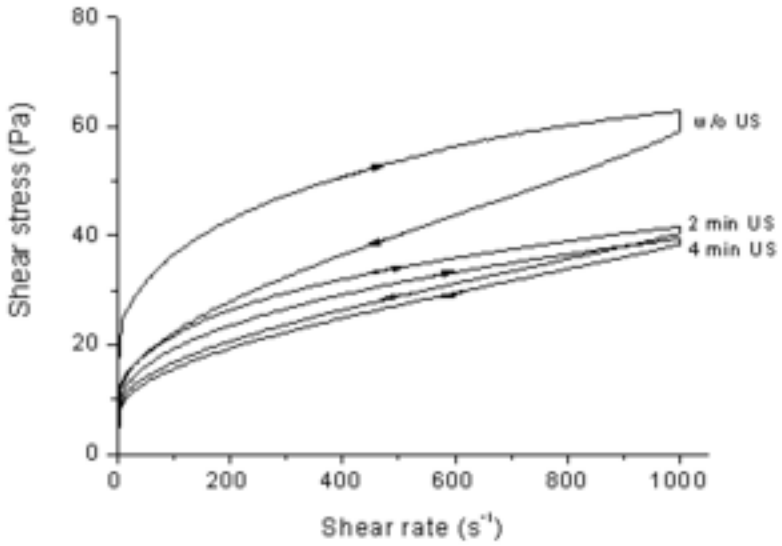

Figure 6. Flow curves of 30 vol.% suspensions of TZ3Y zirconia (Tosoh) with 1 wt% of deflocculant prepared without and with sonication for 2, and 4 min.

Figure
Click here to download high resolution image

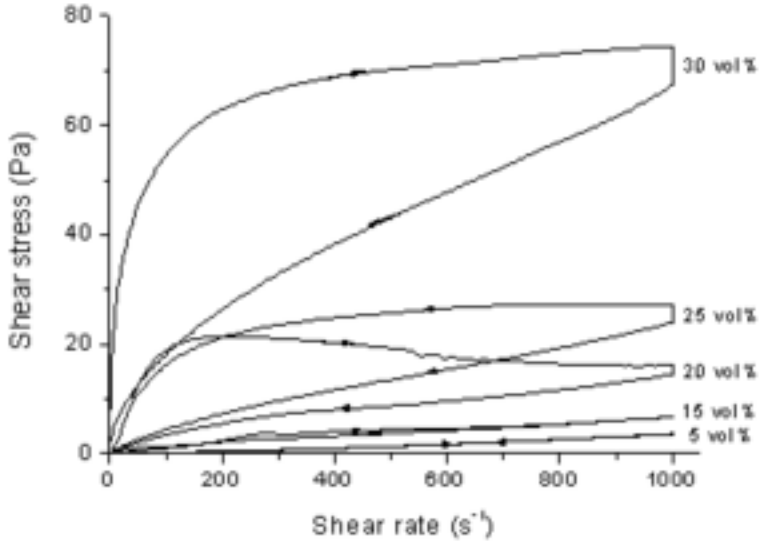

Figure 7. Flow curves suspensions of mixtures of TZ3Y zirconia (Tosoh) and colloidal zirconia (MEL) prepared without sonication to different solids loadings (5-30 vol.%).

Figure
Click here to download high resolution image

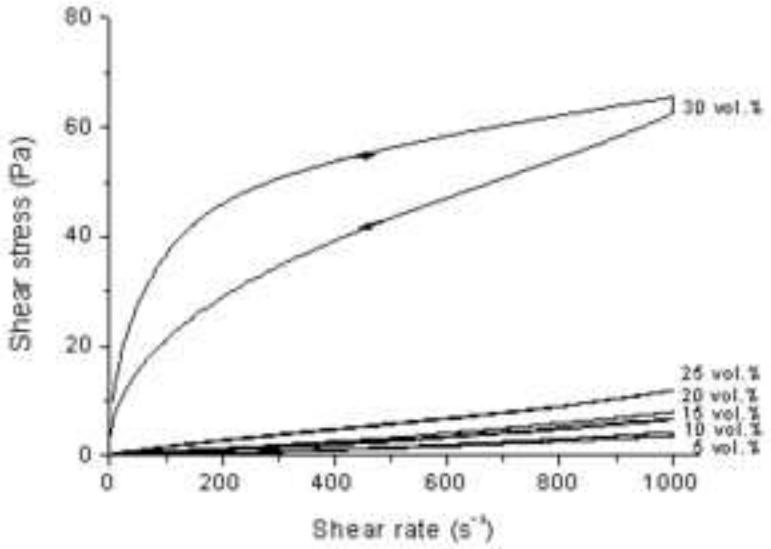

Figure 8. Flow curves suspensions of mixtures of TZ3Y zirconia (Tosoh) and colloidal zirconia (MEL) prepared with 2 min sonication to different solids loadings (5-30 vol.%).

Figure
Click here to download high resolution image

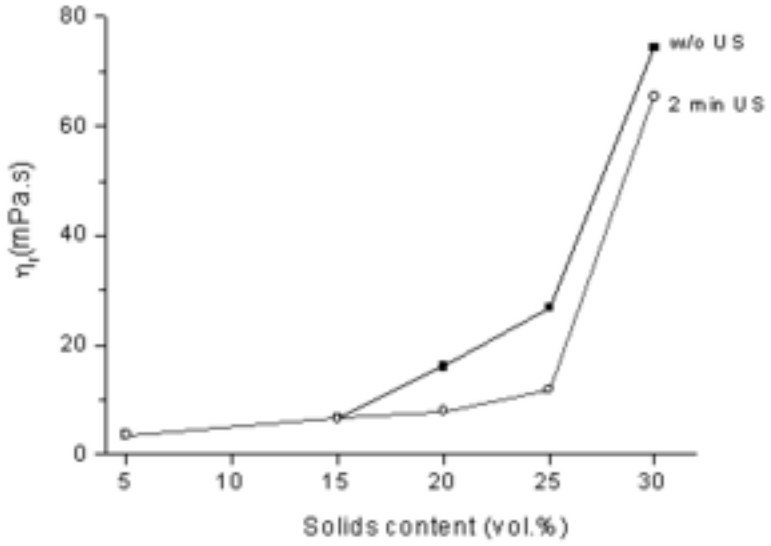

Figure 9. Variation of high shear viscosity of suspensions of the mixtures as a function of solids loading, as-prepared and after 2 min sonication (shear rate, 1000 s^{-1}).

Figure

Click here to download high resolution image

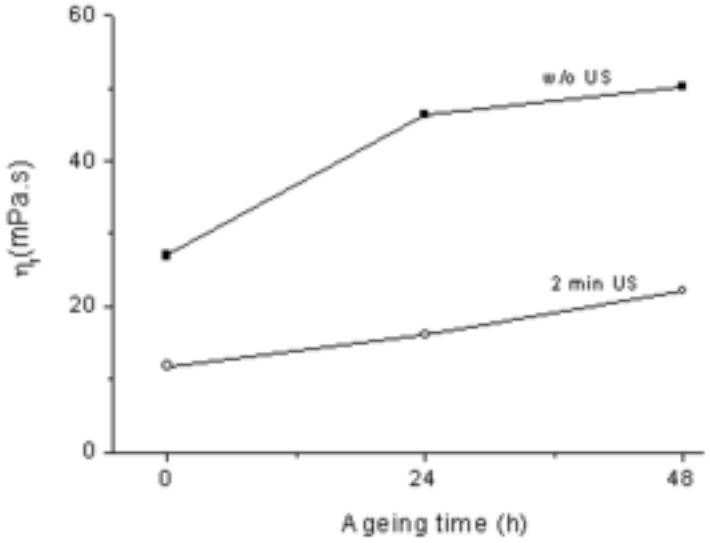

Figure 10. Variation of viscosity with aging time for suspensions with 25 vol.% solids prepared without and with 2 min sonication (shear reate, 1000 s^{-1}).

Figure
Click here to download high resolution image

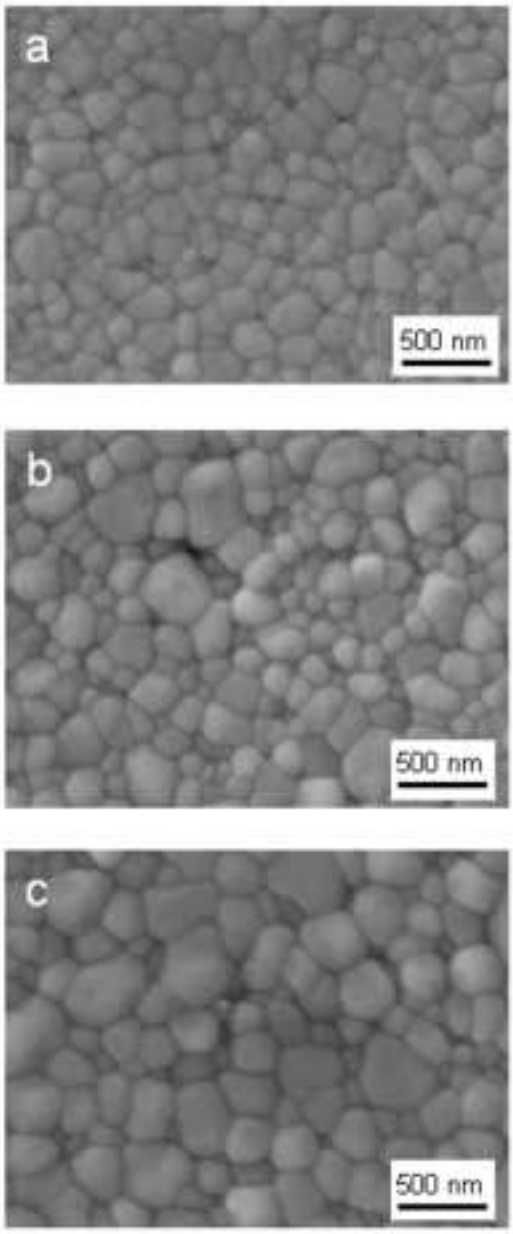

Figure 11. FEG-SEM microstructure of cast specimens sintered at temperatures of 1300°C (a), 1350°C (b), and 1400°C (c).